Available online at www.sciencedirect.com

SciVerse ScienceDirect

Ceramics International 39 (2013) 8087–8095

CERAMICS INTERNATIONAL

www.elsevier.com/locate/ceramint

Size-dependent degradation and bioactivity of borate bioactive glass

Aylin M. Deliormanlı[a,b,*]

[a]Missouri University of Science and Technology, Department of Materials Science and Engineering, and Center for Bone and Tissue Repair and Regeneration, Rolla, MO 65409, USA

[b]Celal Bayar University, Department of Materials Engineering, Muradiye, Manisa, Turkey

Received 21 February 2013; received in revised form 24 March 2013; accepted 25 March 2013
Available online 12 April 2013

Abstract

Borate bioactive glass has been shown to convert faster and more completely to hydroxyapatite and enhances new bone formation in vivo when compared to silicate bioactive glass. In this work, bioactive borate glass scaffolds, with a grid-like microstructure having different filament diameters (130 ± 10 μm to 300 ± 20 μm), were prepared by a robotic deposition technique. In vitro degradation and hydroxyapatite formation on borate bioactive glass scaffolds were investigated in a simulated body fluid (SBF) at 37 °C under static conditions. Mineralization of borate and silicate bioactive glass powders was also tested under the same conditions. When immersed in SBF, degradation rate of the scaffolds and conversion to a hydroxyapatite-like material showed dependence on filament diameter. Similarly, conversion of bioactive glass particles to calcium phosphate phase strongly depends on the particle size and the sample/SBF ratio of the system. Large particles and scaffolds composed of thick struts formed less apatite and degraded less completely compared with smaller particles and thinner struts. Results showed that it is possible to tailor the degradation rate and bioactivity by changing the filament diameter of the borate bioactive glass scaffolds produced by robocasting.

Keywords: Bioactive glass; Scaffolds; Interfaces; Biomedical applications; Tissue engineering

1. Introduction

Porous three-dimensional scaffolds composed of biomaterials are receiving considerable interest for bone tissue engineering applications [1–4]. They represent templates for in vitro culturing of the cells from the patient for the beginning of bone formation. Bioactive glass is a promising scaffold material for bone tissue engineering applications. Silicate bioactive glasses such as 45S5 glass, and compositions based on 45S5 bioglass, such as 13-93 have been widely investigated [5–9]. 45S5 bioactive glass is nowadays used successfully in middle ear and dental implants but it has potential to be used in many more applications [9]. More recently, some borate-based glasses have also been shown to be bioactive [10–13]. Scaffolds of borate bioactive glass designated 13-93B3, a composition formed by replacing all of the SiO_2 in 13-93 with B_2O_3, have been shown to convert faster to HA and to support faster bone growth in rat calvarial defects when compared to scaffolds of silicate 13-93 glass with the same microstructure [14]. In a recent study [15] 45S5 bioglass powder, borosilicate and borate bioactive glass scaffolds were evaluated in critical-sized rat calvarial defects. Results showed that 45S5 and 13-93B3 converted completely to HA in vivo and 13-93B3 glass provided greater bone formation and may be more promising for bone defect repair due to its capacity to be molded into scaffolds [15].

For a given biomaterial composition, the important microstructural characteristics that influence the performance of the scaffold are the porosity, pore size, pore shape and interconnectivity of the pores [16–19]. The porous structure is crucial for migration and proliferation of cells and tissue formation [20]. Similarly, degradation behavior of porous scafffolds plays an important role in the new tissue formation. Degradation properties are of critical importance for biomaterial selection and design as well as the long term success of a tissue engineered construt [21]. Once implanted in the body, a porous scaffold should maintain mechanical strength and structral integrity until the loaded cells adapt to the

*Correspondence address: Celal Bayar University, Department of Materials Engineering, Muradiye Kampusu, Manisa-Turkey.
Tel.: +90 236 2012405; fax: +90 236 2412143.
E-mail addresses: aylin.deliormanli@cbu.edu.tr, deliormanli@mst.edu.

0272-8842/$ - see front matter © 2013 Elsevier Ltd and Techna Group S.r.l. All rights reserved.
http://dx.doi.org/10.1016/j.ceramint.2013.03.081

environment and excrete sufficient amount of extracellular matrix. It is believed that the optimum in vivo degradation rate may be similar or slightly less than the rate of tissue formation. Because the space occupied by porous scaffold is replaced by newly formed tissue [22]. The degradation of scaffolds depends on several parameters, namely the biomaterials intrinsic properties and the scaffold morphology [19–22]. Therefore, the appropriate design of a porous architecture is necessary for tissue engineering reconstruction.

An influence of scaffold architecture on degradation has been widely investigated. For example, Saito et al. [23] investigated the strut size effects on long-term in vivo degradation in poly(L-lactic acid) (PLLA) 3-D scaffolds. Three types of porous PLLA scaffolds with variable pore sizes, strut sizes, porosities, and surface areas were fabricated and implanted subcutaneously into mice. Among the porous scaffolds, the group with the largest strut size lost weight in terms of percentage faster than the other two groups. Scaffold porosity was not found to be significantly correlated with the degradation rate [23]. Deliormanlı et al. [24] investigated the effect of the pore size of borate 13-93B3 bioactive glass scaffolds on the ability to support tissue ingrowth in a rat subcutaneous implantation model. Scaffolds with a grid-like microstructure with the same strut size but having 3 different pore widths were prepared using a robotic deposition technique, and implanted in rats. Results showed that qualitatively, the difference in pore size had little effect on the amount of fibrous tissue infiltrated into the borate glass scaffolds. Additionally, degradation rate of the scaffolds with large pore widths was higher compared to the scaffolds with a smaller one, which was clearly correlated with the porosity difference of the scaffolds [24]. Previously, it was also shown that scaffold/SBF volume ratio strongly affects the degradation rate of borate (13-93B3) scaffolds in vitro [25]. Similarly, Fu and co-workers examined the relationship between bioactive glass scaffold architecture and the degradation behavior. However, in their studies, porous scaffolds were sponge-like whose internal architectures, especially the strut size, could not be precisely controlled [26–28].

The effect of the strut size on the degradation behavior and bioactivity of bioactive glass scaffolds has not been investigated yet systematically. The goal of this study was to investigate the influence of filament size, on the in vitro degradation and bioactivity of the designed bioactive glass scaffolds produced by robocasting. HA formation ability of borate and silicate bioactive glass powders having different particle sizes was also investigated for comparison purposes.

2. Experimental work

2.1. Materials

Borate and silicate bioactive glass, with the composition given in Table 1, was kindly supplied by Mo-Sci Corp., Rolla, MO, USA in frit form.

Particles of borate and silicate bioactive glass were prepared by grinding the as-received glass frits for 3 min in a SPEX swing mill (Model 8500, Metuchen, NJ), sieving to obtain particles of size < 100 μm, followed by attrition-milling (Model 01-HD, Union Process, Akron, OH) for 2.5 h using ethanol as the solvent for borate glass and zirconia balls (3 mm) as the milling media. The slurries were dried at 60 °C and the powder was sieved through a 53 μm stainless steel sieve to eliminate the agglomerates resulting from the drying step. A second group of borate bioactive glass particles were prepared by dry ball milling of the coarse (< 100 μm) bioactive glass particles for 7 days using zirconia balls (10 mm) in a plastic container. Particle size analysis (Microtrac 3501; Microtrac Inc, USA) showed a median diameter of 2.3 μm and 13 μm for attrition-milled and ball-milled borate powders, respectively. Similarly, median particle size of the attrition milled silicate glass powders was 2.1 μm. Third group of glass particles was prepared by only grinding the glass frits for 3 min in a SPEX mill. These particles were sieved through a 106 μm stainless steel sieve and particles bigger than 106 μm and smaller than 300 μm were used in the experiments. The median particle size of the sieved borate and silicate bioactive glass particles were measured to be 185 μm and 220 μm, respectively. Table 2 summarizes the size reduction method and the final median diameter of bioactive glass powders used in the experiments.

For the robotic deposition, 13-93B3 suspensions (inks) were prepared using ethanol, organic additives (ethyl cellulose, polyethylene glycol) and bioactive glass powders with a particle size of 2.3 μm. The procedure followed in ink preparation is described elsewhere in detail [29].

2.2. Scaffold preparation

Three dimensional borate based bioactive glass scaffolds were assembled using a robotic deposition apparatus (3D Inks; Stillwater, OK). For the deposition, the ink was housed in a 3 ml syringe and deposited through a tapered stainless steel nozzle (inner diameter, $D = 200$, 250, 330 and 410 μm) held in a plastic housing (EFD precision tips, East Providence, RI) at a volumetric flow rate required to maintain a constant x-y table speed of 7 mm/s. After printing, the scaffolds were dried under ambient conditions for 24 h, followed by a controlled heat

Table 1
Composition of 13-93 and 13-93B3 glasses (in wt%) used in this work.

Glass	SiO_2	B_2O_3	CaO	Na_2O	K_2O	MgO	P_2O_5
13-93	53		20	6	12	5	4
13-93B3		56.6	18.5	5.5	11.1	4.6	3.7

Table 2
Particle size of the bioactive glass powders utilized in the experiments.

Glass	*Attrition milled* (μm)	*Ball milled* (μm)	*Swing milled* (μm)
13-93	2.1	–	220
13-93B3	2.3	13	185

treatment process. Binder burn out was performed in flowing oxygen using a heating rate in the range of 0.1–1 °C/min. Sintering was performed for 1 h at 560 °C using a heating rate of 5 °C/min. The microstructure of the fabricated scaffolds was examined using scanning electron microscopy; SEM (S-4700, Hitachi, Tokyo, Japan) at an accelerating voltage of 15 kV and a working distance of 12 mm. X-ray diffraction, XRD (Philips XPert, Cu K_α radiation, scanning rate 0.01°/min), was used to investigate for the presence of any crystalline phase in the sintered scaffolds.

2.3. In vitro degradation and bioactivity

The degradation and bioactivity of the scaffolds and bioactive glass particles were investigated in vitro in a simulated body fluid (SBF) under static conditions. SBF was prepared in compliance with the protocol of Kokubo et al. [30], by dissolving reagent-grade chemicals of NaCl, $NaHCO_3$, KCl, $K_2HPO_4 \cdot 3H_2O$, $MgCl_2 \cdot 6H_2O$, $CaCl_2$ and Na_2SO_4 (Sigma Aldrich, USA) in deionized water and buffering at a pH of 7.40 with tris(hydroxymethyl)aminomethane ($(CH_2OH)_3CNH_2$) and 1 M hydrochloric acid (Fisher Scientific Inc., USA) at 37 °C. Table 3 gives the composition of the SBF.

The weight loss of the scaffolds and variation in pH (initial pH =7.4) of SBF were measured after a certain time period to determine the rate and the extent of the conversion. Three different sample/SBF (S/S) ratios (1, 2 and 10 mg/ml) were used in the experiments. Each sample (scaffold or bioactive glass particles) was immersed in a polyethylene bottle containing the SBF solution and kept for up to 60 days without shaking in an incubator at 37 °C. Three scaffolds were used for each immersion time. After removal from the SBF, samples were washed with deionized water, dried at 60 °C overnight and weighed. Degradation degree (weight loss, %) of the scaffolds was estimated simply as

$$(W\%) = (W_0 - W_f)/W_0$$

where W_0 is the initial mass of the scaffold and the W_f is the final mass. Additionally, after the scaffolds were removed from the bottle, the SBF solution in the bottle was cooled to room temperature, and its pH was measured using a pH meter.

Fourier transform infrared spectroscopy (FTIR, Nexus 870, Thermo Nicolet) was used to determine the HA-like layer formation on the surfaces of the scaffolds and glass particles. The reacted dry powders were mixed with KBr at high purity and dry pressed prior to measurements. FTIR was performed in the wave number range of 400–4000 cm^{-1} on disks. During the experiments, the number of scans and the resolution was recorded as 32 and 4 cm^{-1}, respectively. SEM and XRD were used to analyze the microstructure and crystalline phase of the reacted scaffolds and powders, using the conditions described previously.

Table 3
Ion concentration (mM) in SBF and human blood plasma [30].

Ion	Na^+	K^+	Mg^{+2}	Ca^{+2}	Cl^-	HCO_3^-	HPO_4^{-2}	SO_4^{-2}
SBF	142.0	5.0	1.5	2.5	147.8	4.2	1.0	0.5
Human Plasma	142.0	5.0	1.5	2.5	103.0	27.0	1.0	0.5

3. Results and discussions

3.1. Bioactive glass scaffolds

The particle size distribution and SEM images of the attrition-milled and ball-milled borate 13-93 B3 bioactive glass particles are shown in Fig. 1(a and b), respectively. Both types of particles have an angular geometry and a wide distribution of sizes, with a median diameter (d_{50}) of 2.3 μm and 13 μm, respectively. SEM characterization results also indicated that the coarser borate glass particles (185 μm) and silicate glass particles have a similar morphology (not shown).

Fig. 2 shows the digital images of a sintered borate bioactive glass scaffold with a 300 ± 20 μm filament diameter before (a) and after treatment in SBF for 30 days (b and c). From the images, it is clear that the surface and the interior of the scaffold was covered with a second phase material, presumably a calcium phosphate. However, glass phase did not completely convert to this second phase material.

The external shape and grid-like microstructure formed in the robocasting step were retained after the binder burnout and sintering steps and the glass struts (filaments) were almost fully dense. The linear shrinkage of the scaffolds during sintering was almost isotropic, in the range of 25–30%. The pore width, strut diameter and the porosity (as determined from the final mass and external dimensions) of the sintered scaffolds are tabulated in Table 4. Accordingly, strut diameter of the

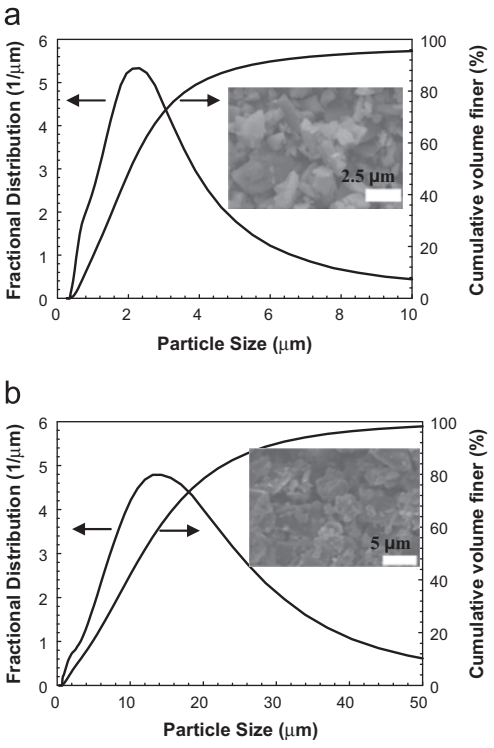

Fig. 1. Particle size distribution and the SEM images of the (a) attrition-milled and (b) ball-milled 13-93B3 bioactive glass particles.

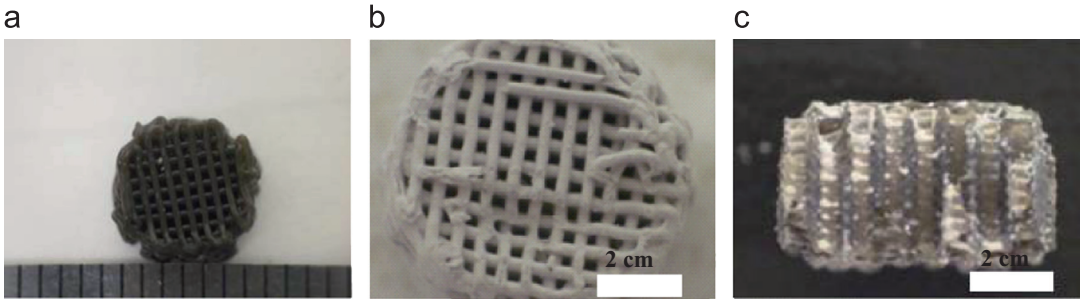

Fig. 2. Digital images of the sintered borate bioactive glass scaffold with a filament diameter of 300 μm: (a) un-treated and (b), (c) treated in SBF for 30 days.

Table 4
Physical properties (pore width, strut diameter and porosity) of 13-93B3 grid-like scaffolds.

Strut diameter (μm) (*during printing*)	*Pore width* (μm) (*after sintering*)	*Strut diameter* (μm) (*after sintering*)	*Porosity* (%) (*after sintering*)
410	420 ± 30	300 ± 20	48 ± 3
330	560 ± 20	230 ± 15	55 ± 2
250	640 ± 40	180 ± 20	60 ± 3
200	750 ± 50	130 ± 10	65 ± 4

sintered scaffolds was ranged from 130 ± 10 to 300 ± 20 μm and the porosity values were between 65 ± 4% and 48 ± 3%. XRD analysis showed no measurable crystallization of the glass after the sintering step (results not shown).

When immersed in an aqueous phosphate solution, such as the body fluid, bioactive glasses convert to an amorphous calcium phosphate or hydroxyapatite (HA)-like material, which is responsible for their strong bonding with surrounding tissue [5–8,10,31,32]. In the present study, the bioactivity of the borate glass was evaluated in vitro in SBF. The degradation and conversion of the borate bioactive glass scaffolds to HA in a SBF occurs by dissolution of components such as Na_2O, K_2O, and B_2O_3 into the solution to form Na^+, K^+, $(BO3)^{-3}$, coupled with the reaction of Ca^{+2} ions from the glass with PO_3^{-4} from the solution to form a HA layer on the glass [26,27]. Fig. 3(a and b) shows the weight loss values of the scaffolds with various filament size prepared by robocasting and pH of the SBF solution as a function of immersion time, respectively. Results revealed that the weight loss percentage of the borate 13-93B3 scaffolds with a filament diameter of 130 ± 10 μm, and the pH of the corresponding SBF solution was higher than the related values of the scaffolds having a larger filament diameter. After immersion for 60 days, the weight loss reached 53% ± 2 for scaffolds with a filament diameter of 300 ± 20 μm. However, weight loss was found 60% ± 3 for the scaffolds with a filament diameter of 180 ± 20 μm and it was 67% ± 1 for the scaffolds having a filament diameter of 130 ± 10 μm. If it is assumed that ions such as Na^+, K^+, $(BO3)^{-3}$, dissolve in the solution and that all the CaO in the glass reacts with the phosphate ions in the SBF to form HA,$Ca_{10}(PO_4)_6(OH)_2$, then the theoretical weight loss of the fully converted glass scaffolds is 67%. The lower value

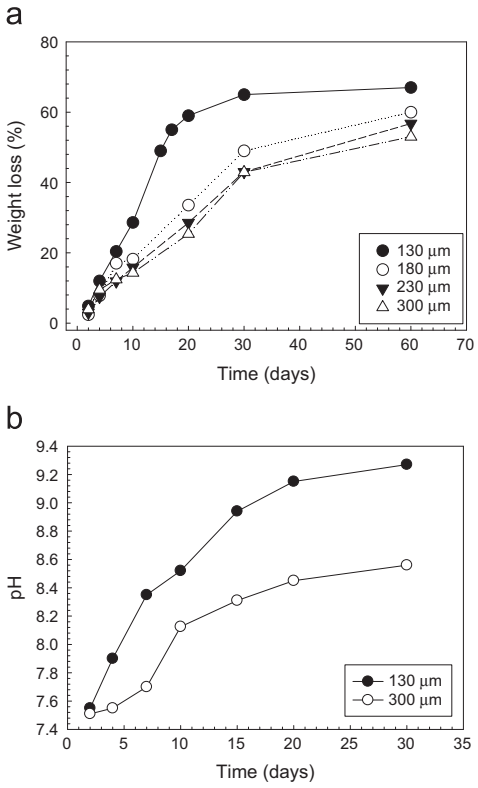

Fig. 3. (a) Weight loss of 13-93B3 bioactive glass scaffolds in SBF solution (10 mg/ml) as a function of strut diameter, (b) the pH of the SBF solutions as a function of immersion time of 13-93B3 scaffolds.

of the measured weight loss of the thicker scaffolds compared to the theoretical value may indicate that the borate 13-93B3 scaffolds (with a strut diameter of ~300, 230 and 180 μm) did not completely convert to HA after the 60-day immersion.

The pH of the SBF (initial value = 7.4) increased with time upon immersion of the bioactive glass scaffolds. After immersion of the scaffolds for 30 days, the pH of the SBF increased to 9.26 and 8.56 for the scaffolds with a strut diameter of 130 ± 10 μm and 300 ± 20 μm, respectively. The change in pH of the SBF was attributed to the dissolution of boron (presumably as borate ions) and the network modifiers (such as Na^+ and K^+) during the degradation of the glass, coupled with the consumption of phosphate ions from the solution in the formation of the HA-like product.

Results also showed that the weight loss values of the scaffolds with a strut diameter of 130 ± 10 μm and the increase in pH of the SBF solution was significantly high compared to the other scaffolds. Even in the case of scaffolds having a strut diameter of 180 ± 20 μm, lower degradation rates were observed compared to the scaffolds with 130 ± 10 μm strut diameter. The reason of the high degradation rates of scaffolds starting from this critical size (strut size 130 ± 10 μm) is not clear yet.

Porosity is also an important factor which tailors the degradation rate of the tissue engineering scaffolds [20]. However, in the current study, porosity of the prepared scaffolds was between $48\% \pm 3$ and $65\% \pm 4$. Therefore, the difference obtained in degradation rates of the borate glass scaffolds cannot be totally attributed to the porosity difference. Previous study of Deliormanlı and Rahaman [29] showed that 13-93B3 cubic scaffolds having a ~300 μm strut size with ~50% porosity did not degrade completely and convert to HA-like material in 30 days. After 60 days in SBF, the weight loss of the borate 13-93B3 scaffolds was $56\% \pm 6$ (Theoretical weight loss 67%) and the surface of the scaffolds was still covered by amorphous calcium phosphate (ACP) layer. On the other hand, previous study of Fu et al. [27] showed that degradation rate of 13-93B3 scaffolds prepared by polymer foam replication (having strut size about 100 μm, porosity 78–82%; pore size 100–500 μm) was $67\% \pm 2$ after 200-hour immersion in SBF (10 mg/ml S/S ratio). Therefore, it is possible to conclude that strut size has a strong influence on the degradation rate of bioactive glass scaffolds. Additionally, this effect may be more significant starting from a critical size.

SEM images in Fig. 4 show the surfaces of the borate 13-93B3 scaffolds with a filament diameter of 130 ± 10 μm and 300 ± 20 μm after immersion in SBF for 30 days. When compared to the smooth surface of the sintered scaffolds, the surface of the reacted scaffolds had a fine particulate structure. Converted layer on the scaffolds was composed of rounded particles, which is consistent with the information reported previously for 13-93B3 glass [26,27]. A significant difference was not observed on the morphology and the particle size of the converted material depending on the strut diameter.

Fig. 5 demonstrates the FTIR spectra of the powders obtained from the surface (converted region) of the scaffolds treated in SBF (10 mg/ml) for 30 days. The spectrum of the as-prepared 13-93B3 glass powder is also shown for comparison purposes. For the un-treated glass powder resonances shown at 1440 cm^{-1} and 730 cm^{-1} were assigned to the B–O stretching mode and bending mode of BO_3 groups, respectively. The resonance at 1050 cm^{-1} was assigned to the B–O stretching mode of BO_4 group. FTIR spectroscopy of the scaffolds showed resonances at 1000–1100 cm^{-1} and at 570 cm^{-1} corresponding to a calcium phosphate [31,33]. The resonances at 1390 cm^{-1} were attributed to C-O in the $(CO_3)^{2-}$ group. After immersion in SBF the resonances attributed to the 13-93B3 glass network weakened and resonances attributed to the vibrations of the phosphate group dominated the spectrum. Results also indicate that the converted layer might be an amorphous calcium phosphate (ACP) material, presumably a

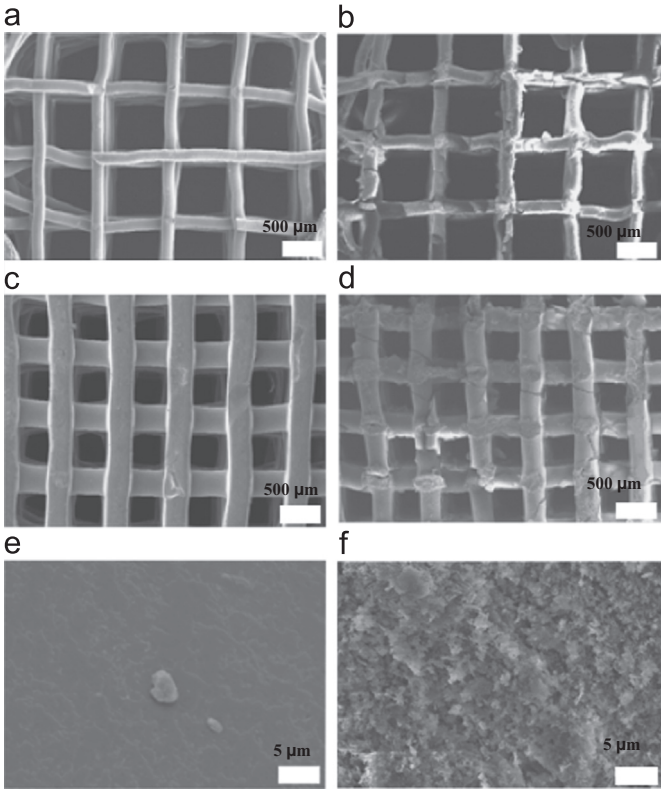

Fig. 4. SEM images of the bioactive glass scaffolds with a filament diameter of 130 μm and 300 μm: un-treated and (b,d,f) after treatment in SBF (10 mg/ml), for 30 days.

precursor to the formation of the crystalline HA phase. It is known that ACP is formed on the surface of bioactive glass at the initial stage of conversion in SBF. Ca^{2+} deficient HA was then formed by crystallization of ACP [34]. In the current study, no significant difference was observed in the FTIR spectra of the powders obtained from the converted layer of scaffolds depending on the filament diameter. However, peak intensities of the sample corresponding to the scaffold with a filament diameter of 130 ± 10 μm were high compared to the other samples. Additionally, there was a resonance at 866 cm^{-1} corresponding to the stretching vibration of CO_3^{-2} function group which indicated that as formed calcium phosphate had carbonate groups substituted into the structure.

In summary, filament size of the borate scaffolds affected their degradation rate in SBF solution under static conditions. Scaffolds with a filament diameter starting from 130 ± 10 μm degraded much faster compared to the scaffolds having thicker struts such as 300 ± 20 μm. It is confirmed that the filament diameter influences the degradation rate of 13-93B3 robocast scaffolds and their ability to convert to HA.

3.2. Bioactive glass particles

Size-dependent bioactivity of the glass powder particles was investigated under the same conditions with the scaffolds. FTIR spectra of the 13-93B3 powders, which were treated in SBF (10 mg/ml), are shown in Fig.6. Results showed that the intensity of the peaks corresponding to the calcium phosphate

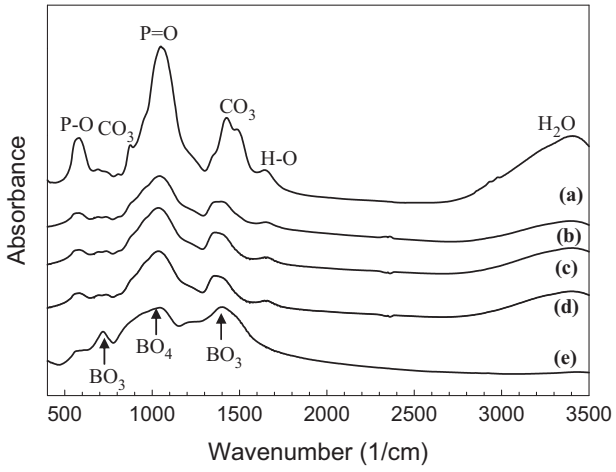

Fig. 5. FTIR spectra of the powders obtained from the surface of 13-93B3 scaffolds immersed in SBF (10 mg/ml) for 30 days: (a) 130 μm, (b) 180 μm, (c) 230 μm, (d) 300 μm, (e) as-prepared 13-93B3 glass powder, as a reference.

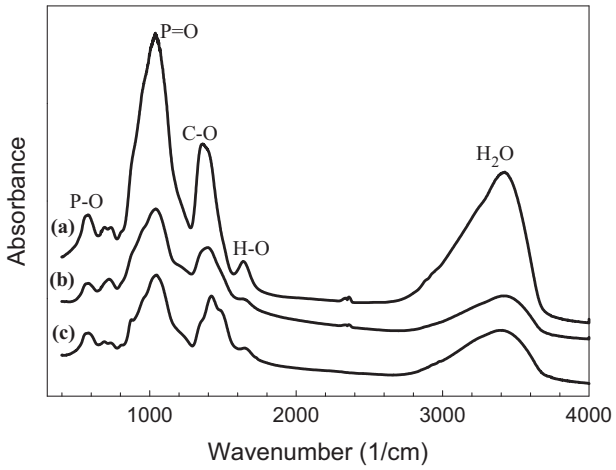

Fig. 6. FTIR spectra of 13-93B3 powders after treatment in SBF (10 mg/ml) for 30 days: (a) 2 μm, (b) 13 μm, (c) 185 μm.

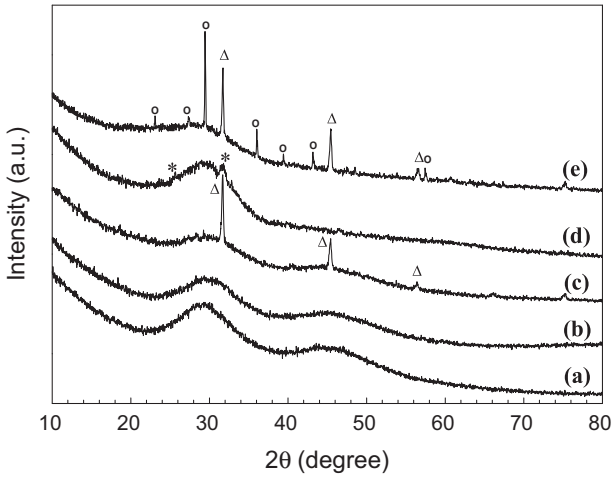

Fig. 7. XRD diagram of silicate and borate glass particles after immersion in SBF (10 mg/ml) for 30 days: (a) un-treated 13-93B3 particle, (b) SBF-treated coarse (185 μm) 13-93B3 particle, (c) SBF-treated fine (2.3 μm) 13-93B3 particle, (d) SBF-treated coarse (220 μm) silicate 13-93 bioactive glass particle, (e) SBF-treated fine (2.1 μm) silicate 13-93 bioactive glass particle (°, Calcite, Δ, Halite, *, HA).

was higher for 2.3 μm particle compared to the coarser particles.

XRD analysis of the 13-93B3 powders with a particle size of 185 μm and 2.3 μm after reaction in SBF (10 mg/ml) for 30 days did not show the presence of a crystalline HA phase (Fig. 7). Instead, the diffraction pattern showed a broad band centered at ∼30° and 45° 2θ in Fig. 7(b). This result is consistent with the experimental findings obtained for the bioactivity of the 13-93B3 scaffolds at the same scaffold/sample (S/S) ratio, which is 10 mg/ml. The major crystalline peaks (at ∼31.8°, 46.4°, 56.4° 2θ) observed (Fig. 7(c)) for the fine borate glass powder corresponds to a reference halite (NaCl) (JCPDS 5-0628), which might have formed due to the residues on the sample after removal from SBF. Unless the samples should not be washed with distilled water thoroughly after removal from SBF, these peaks may be observed due to NaCl crystal (halite) formation on the surface of the sample. On the other hand, XRD diagram of the SBF treated silicate bioactive glass (13-93) powders having the similar particle size (2.1 μm) with borate 13-93B3 showed crystalline phases that corresponds to a calcite $CaCO_3$ (JCPDS 5-0586) together with the halite (Fig. 7(e)). Similarly, XRD diagram of the SBF treated 13-93 powders having larger particle size (220 μm) showed peaks corresponding to the (0 0 2) and (2 1 1) planes in crystalline HA (Fig. 7(d)). No calcite formation was found for the coarser 13-93 powders treated in SBF. Based on these results, it is possible to conclude that surface of the 13-93B3 powders (2.3 to 185 μm) do not convert to crystalline HA in 30 days in a SBF solution having high glass powder concentration (10 mg/ml). On the other hand, XRD results confirmed the formation of a crystalline calcite layer on the surface of the silicate-based bioactive glass 13-93 powders (2.1 μm) and a crystalline HA layer on the surface of coarser (220 μm) 13-93 glass powders under the same conditions. Jones et al. [33] observed calcite formation for 45S5 bioactive glass particles after immersion in SBF. It was found that calcite is forming at the expense of HA for high glass powder concentrations in SBF. Because an excessive amount of calcium ions release in the SBF resulting in a higher Ca/P ratio and a pH shift in SBF and this favors the precipitation of calcite [33]. Furthermore, calcite formation on bioactive glass particles is likely because of the large surface area of the fine particles resulting in an enhanced diffusion of Ca ions in the glass network. Therefore, in the current study calcite formation observed on the fine 13-93 particles may be attributed to the both particle size effect and high particle concentration effect.

In a previous study [25] it was shown that sample/SBF ratio has significant influence on the degredation rate and bioactivity of 13-93B3 scaffolds and powders. The zeta potential values of the borate glass particles (∼2 μm) after immersion in SBF (10 mg/ml) were still positive after 30 days. On the other hand, at lower S/S ratios (such as 1 mg/ml) a negative surface charge developed on the particles. The sign reversal observed in

powders immersed in SBF was attributed to the HA formation on the surface [25]. Fig. 8 shows the XRD diagram of the 13-93B3 powders (2.3 μm) immersed in SBF (at different S/S ratios) for 30 days. Results revealed that borate bioactive glass powders (2.3 μm) can convert to crystalline HA only at 2 mg/ml and 1 mg/ml S/S ratios in 30 days. Peak broadening observed in Fig. 8(a and b) may be attributed to the formation of HA particles with a very small particle size. Peaks became sharper in Fig. 8(a) because of the crystal growth. Halite also has a characteristic peak at the same degree with the major peak of crystalline HA (Fig. 8(c)). XRD analysis shown in Fig. 9 also confirms crystalline HA formation on the surface of both fine borate and silicate bioactive glass powders treated in SBF (1 mg/ml) just after 3 days.

On the other hand, if the particle size of the powder is increased (185 μm), HA formation can be achieved only at a ratio of 1 mg/ml SBF (see Fig. 10) after a longer period. In Fig. 10, major resonances (P–O bending vibration) associated

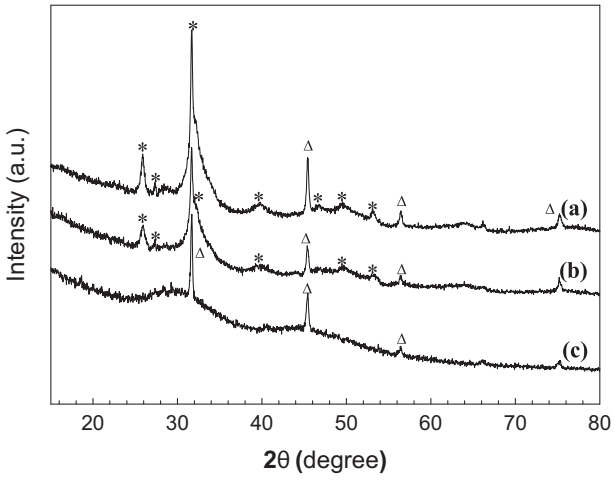

Fig. 8. XRD diagram of the fine 13-93B3 particles (2.3 μm) after treatment in SBF at different S/S ratios for 30 days: (a) 1 mg/ml, (b) 2 mg/ml, (c) 10 mg/ml (*, HA; Δ, Halite).

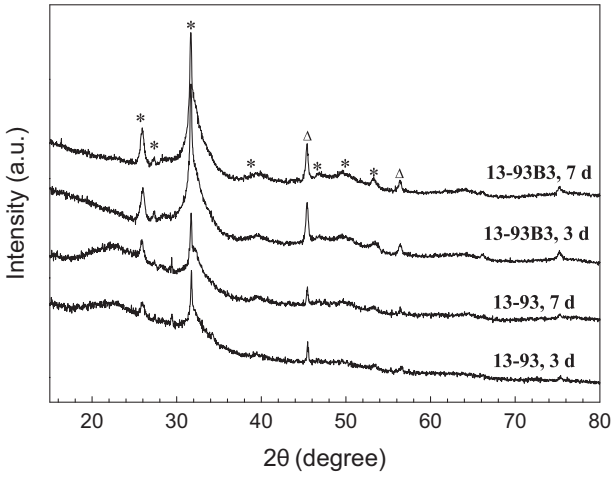

Fig. 9. XRD diagram of the 13-93B3 and 13-93 bioactive glass particles (~2 μm) after treatment in SBF (1 mg/ml) for 3 and 7 days (*, HA; Δ, Halite).

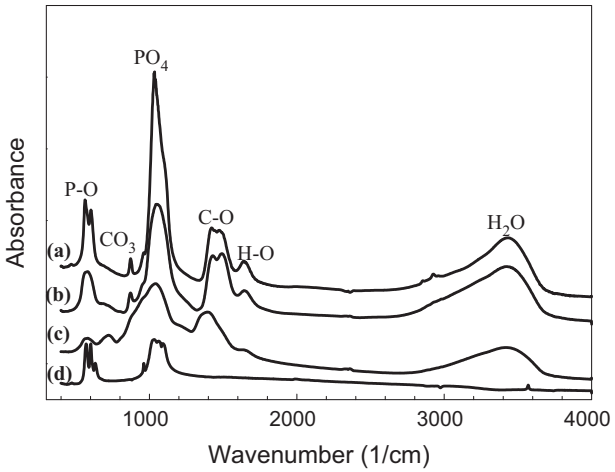

Fig. 10. FTIR spectra of the coarse 13-93B3 particles (185 μm) after treatment in SBF at different S/S ratios for 30 days: (a) 1 mg/ml, (b) 2 mg/ml, (c) 10 mg/ml, (d) HA powder as reference.

with crystalline HA at wave numbers of 560 and 603 cm^{-1} were observed for the bioactive glass samples soaked in SBF (1 mg/ml) for 30 days but not for the as prepared glass providing indication for the formation of an HA layer on the surface of the glass samples. This means that in regards to the coarser particles, the amount of calcium and phosphate ions in the medium per gram of the samples should be high enough for crystalline HA formation to occur.

Previously, Cerruti [35] analyzed the dissolution of Bioglass (45S5) samples of average particle size of 2, 16 and 90 μm in TRIS-buffer. As for smaller particles, cation release was faster, higher values of pH were reached, and a thinner layer of calcium phosphate was formed. The final concentration of Si in solution was not affected by particle size [35]. Similarly, Zhang and co-workers [36] investigated the influence of particle size of bioactive glasses in vitro. Large particles (600 μm < large < 1000 μm) formed less apatite and degraded less completely compared with small (212 μm < small < 355 μm) particles. Another study performed by Zhang and co-workers [37] showed that the particle size had a strong impact on the in vitro behavior of the glasses. Larger particles showed a smaller increase in pH but more clear reaction layers than particles smaller than 250 μm. Generally, the average thickness of overall reaction layer, decreased with the total surface area of the sample, i.e. with decreasing particle size. It was found that the finer the fraction, the poorer the diffusion between the solution inside the particle bed and the bulk solution, thus yielding less-developed reaction layers on the particles inside the bed [37]. Similar phenomena have been observed by Greenspan et al. [38]. According to their work, higher S/S ratios gave faster and larger increases in pH and rapid initial layer formation, but less-developed calcium phosphate layers than lower S/S ratios [38]. More recently, Mackovic et al. [39] investigated the nanoscale reactivity and biocompatibility of 45S5 nanoparticles. They observed formation of a nanocrystalline and large calcite because of higher reactivity of nano bioactive glass particles in comparison to conventional micron sized bioactive glass particles [39].

Based on the previous studies reported in literature and the results of the current work it is clear that for smaller bioactive glass particles, the dissolution and reaction rate with the medium was faster. Results also showed that particle size has some influence on the in vitro conversion of bioactive glass to crstalline HA phase. For fine 13-93B3 particles (2.3 μm), 2 mg/ml S/S ratio was sufficient for conversion of the bioactive glass to HA. However, for coarser 13-93B3 particles (185 μm), lower S/S ratios (1 mg/ml) was necessary to obtain crystalline phase.

4. Conclusions

Borate based bioactive glass scaffolds with a grid-like microstructure and having different filament diameters (130 ± 10 μm to 300 ± 20 μm) were prepared by a robotic deposition technique. In vitro degradation and hydroxyapatite formation on borate bioactive glass scaffolds were investigated in SBF at different S/S ratios 37 °C up to two months under static conditions. Mineralization of borate bioactive glass powders were also tested under the same conditions for comparison purposes. Results showed that 13-93B3 powders (2.3, 13 and 185 μm) do not convert to crystalline HA in 30 days in a SBF solution at 10 mg/ml S/S ratio. With respect to fine 13-93B3 bioactive glass particles (2.3 μm), 2 mg/ml S/S ratio was sufficient whereas, for coarser 13-93B3 particles (185 μm), lower S/S ratios (1 mg/ml) were required for conversion of the bioactive glass to HA. Scaffolds with a filament diameter starting from $130 \pm$ μm degrade much faster compared to the scaffolds having thicker struts. All scaffolds (filament diameters from 130 ± 10 μm to 300 ± 10 μm) were converted to amorphous calcium phosphate material after 30 days of immersion in SBF. Results of this study showed that it is possible to tailor the degradation rate by changing the filament diameter of the scaffolds produced by robocasting. Tailoring the filament diameter may be a useful tool to adjust the scaffold degradation to a specific application without the need to change the material composition.

Acknowledgments

The author would like to thank Hailuo Fu and Xin Liu for technical assistance, and Mo-Sci Corp., Rolla, for supplying the bioactive glass. Support and useful discussions by Prof. Mohamed N.Rahaman is greatly appreciated. The financial support for this research was provided by the Center for Bone and Tissue Repair and Regeneration at Missouri University of Science and Technology, and by The Scientific and Technical Research Council of Turkey in the form of a TUBITAK-BIDEB 2219 fellowship.

References

[1] T.M.G. Chu, D.G. Orton, S.J. Hollister, S.E Feinberg, J.W. Halloran, Mechanical and in vivo *p*erformance of hydroxyapatite implants with controlled architectures, Biomaterials 23 (2002) 1283–1293.

[2] E Charriere, J Lemaitre, P. Zysset, Hydroxyapatite cement scaffolds with controlled macroporosity: fabrication protocol and mechanical properties, Biomaterials 24 (2003) 809–817.

[3] O Gauthier, J.M. Bouler, E Aguado, P. Pilet, G. Daculsi, Macroporous biphasic calcium phosphate ceramics: influence of macropore diameter and macroporosity percentage on bone ingrowth, Biomaterials 19 (1998) 133–139.

[4] D. Zhang, H. Jain, M. Hupa, L. Hupa, In-vitro degradation and bioactivity of tailored amorphous multi porous scaffold structure, Journal of the American Ceramic Society 95 (2012) 2687–2694.

[5] L.L. Hench, Bioactive materials: the potential for tissue regeneration, Journal of the Biomedical Materials Research 15 (1998) 511–518.

[6] M. Brink, T. Turunen, R. Happonen, A. Yli-Urppo, Compositional dependence of bioactivity of glasses in the system Na_2O–K_2O–MgO–CaO–B_2O_3–P_2O_5–SiO_2, Journal of Materials Science Materials in Medicine 37 (1997) 114–121.

[7] L.-C. Gerhardt, A.R. Boccaccini, Bioactive glass and glass-ceramic scaffolds for bone tissue engineering, Materials 3 (2010) 3867–3910.

[8] M.N. Rahaman, D.E. Day, B.S. Bal, Q. Fu, S.B. Jung, L.F. Bonewald, Bioactive glass in tissue engineering, Acta Biomaterialia 7 (2011) 2355–2373.

[9] D.U. Tulyaganov, M.E Makhkamov, A. Urazbaev, A. Goel, J.M. F. Ferreira, Synthesis, processing and characterization of a bioactive glass composition for bone regenaration, Ceramic International 39 (2013) 2519–2526.

[10] D.E Day, J.E White, R.F. Brown, K.D. McMenamin, Transformation of borate glasses into biologically useful materials, Glass Technology Part A 44 (2003) 75–81.

[11] X. Liu, Z. Xie, C. Zhang, H. Pan, M.N. Rahaman, X. Zhang, Q. Fu, W. Huang, Bioactive borate glass scaffolds: in vitro and in vivo evaluation for use as a drug delivery system in the treatment of bone infection, Journal of Materials Science Materials in Medicine 21 (2010) 575–582.

[12] A Yao, D. Wang, W. Huang, Q. Fu, M.N. Rahaman, D.E. Day, In vitro bioactive characteristics of borate-based glasses with controllable degradation behavior, Journal of the American Ceramic Society 90 (2007) 303–306.

[13] Q. Fu, M.N. Rahaman, H. Fu, X. Liu, Silicate, borosilicate, and borate bioactive glass scaffolds with controllable degradation rate for bone tissue engineering applications. I. Preparation and in vitro degradation, Journal of Biomedical Materials Research Part A 95A (2010) 164–171.

[14] S. Jung, Borate Based Bioactive Glass Scaffolds for Hard and Soft Tissue Engineering, Ph.D. Dissertation, Missouri University of Science and Technology, 2010.

[15] L. Bi, S. Jung, D. Day, K. Neidig, V. Dusevich, D Eick, L. Bonewald, Evaluation of bone regeneration, angiogenesis, and hydroxyapatite conversion in critical-sized rat calvarial defects implanted with bioactive glass scaffolds, Journal of Biomedical Materials Research Part A 100 A (2012) 3267–3275.

[16] B Feng, Z. Jinkang, W. Zhen, L. Jianxi, C. Jiang, L. Jian, M. Guolin, D. Xin, The effect of pore size on tissue ingrowth and neovascularization in porous bioceramics of controlled architecture in vivo, Biomedical Materials 6 (2011) 1–10.

[17] M. Rumpler, A. Woesz, J.W.C. Dunlop, J.T. Van Dongen, P. Fratzl, The effect of geometry on three-dimensional tissue growth, Journal of the Royal Society Interface 5 (2008) 1173–1180.

[18] B.S. Chang, C.K Lee, K.S Hong, H.J. Youn, H.S. Ryu, S.S. Chung, Osteoconduction at porous hydroxyapatite with various pore configurations, Biomaterials 21 (2000) 1291–1298.

[19] J.X. Lu, B. Flautre, K. Anselme, P. Hardouin, A. Gallur, M. Descamps, B. Thierry, Role of interconnections in porous bioceramics on bone recolonization in *v*itro and in vivo, Journal of Materials Science: Materials in Medicine 10 (1998) 111–120.

[20] V Karageorgiaou, D.L. Kaplan, Porosity of 3-D biomaterial scaffolds and osteogenesis, Biomaterials 26 (2005) 5474–5491.

[21] H-J. Sung, C. Meredith, C. Johnson, Z.S Galis, The effect of scaffold degradation rate on the three dimensional cell growth and angiogenesis, Biomaterials 25 (2004) 5735–5742.

[22] L Wu, J. Ding, In vitro degradation of three-dimensional porous poly(D,L-lactide-co-glycolide) scaffolds for tissue engineering, Biomaterials 25 (2004) 5821–5830.
[23] E. Saito, Y. Liu, F. Migneco, S. J. Hollister, Strut size and surface area effects on long-term in vivo degradation in computer designed poly(L-lactic acid) three-dimensional porous scaffolds, Acta Biomaterialia 8 (2012) 2568–2577.
[24] A.M. Deliormanli, X. Liu, M.N. Rahaman, Evaluation of borate bioactive glass scaffolds with different pore sizes in a rat subcutaneous implantation model, Journal Biomaterials Applications http://dx.doi.org/10.1177/0885328212470013.
[25] A.M. Deliormanli, In vitro assesment of degradation and bioactivity of robocast bioactive glas scaffolds in simulated body fluid, Ceramic International 38 (2012) 6435–6444.
[26] H. Fu, Q. Fu, N. Zhou, W. Huang, M.N. Rahaman, D. Wang, X. Liu, In vitro evaluation of borate-based bioactive glass scaffolds prepared by a polymer foam replication method, Materials Science and Engineering C 29 (2009) 2275–2281.
[27] Q. Fu, M.N. Rahaman, H. Fu, X. Liu, Silicate, borosilicate, and borate bioactive glass scaffolds with controllable degradation rate for bone tissue engineering applications. I. Preparation and in vitro degradation, Journal of Biomedical Materials Research Part A 95A (2010) 164–171.
[28] Q. Fu, M.N Rahaman, S. Bal, K. Kuroki, R.F. Brown, In vivo evaluation of 13-93 bioactive glass scaffolds with trabecular and oriented microstructures in a subcutaneous rat implantation model, Journal of Biomedical Materials Research Part A 95A (2010) 235–244.
[29] A.M. Deliormanlı, M.N Rahaman, Direct-write assembly of silicate and borate bioactive glass scaffolds for bone repair, Journal of the European Ceramic Society 32 (2012) 3637–3646.
[30] T. Kokubo, H. Kushitani, S. Saka, T. Kitsugi, T. Yamamuro, Solutions able to reproduce in vivo surface-structure changes in bioactive glass-ceramic A-W, Journal of Biomedical Materials Research 24 (1990) 721–734.
[31] A Yao, D. Wang, W. Huang, Q. Fu, M.N. Rahaman, D.E. Day, In vitro bioactive characteristics of borate-based glasses with controllable degradation behavior, Journal of the American Ceramic Society 90 (2007) 303–306.
[32] W. Huang, D.E Day, K. Kittiratanapiboon, M.N. Rahaman, Kinetics and mechanisms of the conversion of silicate (45S5), borate, and borosilicate glasses to hydroxyapatite in dilute phosphate solution, Journal of Materials Science Materials in Medicine 17 (2006) 583–596.
[33] J.R. Jones, P. Sepulveda, L.L. Hench, Dose-dependent behavior of bioactive glass dissolution, Journal of Biomedical Materials Research A 58 (2001) 720–726.
[34] H.-M. Kim, T. Himeno, M. Kawashita, T. Kokubo, T. Nakamura, The mechanism of biomineralization of bone like apatite on synthetic hydroxyapatite: an in vitro assessment, Journal of the Royal Society Interface 1 (2004) 17–22.
[35] M.G. Cerrutti, Characterization of Bioactive Glasses; Effect of the Immersion in Solutions that Simulate Body Fluids, Ph.D. Thesis, University of Turin, Department of Chemistry, 2004.
[36] K Zhang, H Yan, D.C. Bell, A Stein, L.F. Francis, Effects of materials parameters on mineralization and degradation of sol-gel bioactive glasses with 3D-ordered macroporous structures, Journal of Biomedical Materials Research 66A (2003) 860–869.
[37] D Zhang, M. Hupa, L. Hupa, In situ pH within particle beds of bioactive glasses, Acta Biomaterialia. 4 (2008) 1498–1505.
[38] D.C Greenspan, I.P. Zhong, G.P. La Torre, Effect of surface area to volume ratio on in vitro surface reactions of bioactive glass particulates, Bioceramics 7 (1994) 55–60.
[39] M Mackovic, A Hoppe, R Detsch, D Mohn, W.J Stark, E Spiecker, A. R Boccaccini, Bioactive glass (type 45S5) nanoparticles: in vitro reactivity on nanoscale and biocompatibility, Journal of Nanoparticle Research 14 (2012) 966–987.